

Unsupervised Manifold Clustering of Topological Phononics

Yang Long, Jie Ren,* and Hong Chen

Center for Phononics and Thermal Energy Science, China-EU Joint Center for Nanophononics,
Shanghai Key Laboratory of Special Artificial Microstructure Materials and Technology,
School of Physics Sciences and Engineering, Tongji University, Shanghai 200092, China

(Dated: November 20, 2021)

Classification of topological phononics is challenging due to the lack of universal topological invariants and the randomness of structure patterns. Here, we show the unsupervised manifold learning for clustering topological phononics without any priori knowledge, neither topological invariants nor supervised trainings, even when systems are imperfect or disordered. This is achieved by exploiting the real-space projection operator about finite phononic lattices to describe the correlation between oscillators. We exemplify the efficient unsupervised manifold clustering in typical phononic systems, including one-dimensional Su-Schrieffer-Heeger-type phononic chain with random couplings, amorphous phononic topological insulators, higher-order phononic topological states and non-Hermitian phononic chain with random dissipations. The results would inspire more efforts on applications of unsupervised machine learning for topological phononic devices and beyond.

Topological phononics unveil complex mechanism behind unconventional phononic wave phenomena [1–7], which lead to the backscattering immune phononic transport modes [8–12], and would be a promising route to the future robust on-chip communication devices [2, 13–17]. To characterize non-trivial phononic topological properties, the key fundamental physical concept is the topological invariant, which is responsible for classifying the topological classes. However, there is NO universal topological invariant for all topological phononic systems. And it is even difficult to properly define them when considering many aspects such as symmetry conditions [17], geometry features [11] and material dispersive responses [12]. Yet, no matter whether topological invariants are well defined or not, topological properties of phononic states are essentially embedded in the global structure features. So far, most of topological invariants are defined based on the Bloch momentum space of the perfect periodic structure [5, 15, 18, 19]. But, these momentum-based approaches will have inevitable shortages or inapplicability when handling with phononic models like the spatial randomness of mechanical parameters, the non-Hermitian features or the amorphous structures. Therefore, finding a general way to explore the topological properties based on real space without defining topological invariants *ad hoc* will be significant but also challenging for the future development of topological phononics and beyond.

Machine learning has shown the power on condensed matters, quantum domains and topological physics [20–24], e.g., the phase learning of quantum many-body systems [25–29], the inverse design of topological optics [30, 31], and the optimization of meta-material devices [32–34]. However, most of these research works focus on the supervised learning, which can not capture the sample features without a priori knowledge and needs extensive samples with well-defined labels. Recently, the unsupervised learning, which can find potential principles behind raw datasets without labels, has been attracting much attention about its ability on phase detections and classifications in spin systems [35–37], particle explorations in high energy physics [38, 39] and efficient material discover-

ies [40]. Therefore, unsupervised machine learning would be the meaningful and powerful way to detect and classify topological properties from abundant phononic structures without any priori knowledge about topological mechanism.

In this Letter, we demonstrate the unsupervised manifold clustering of topological phononics based on similarities of dynamic properties in real space. The real-space dynamic properties of phononic system are represented by its projection operator \hat{P} , which reflects the responses and correlations between oscillators and thus contain the necessary information about the topological properties [41–44]. We firstly show manifold learning can unsupervisedly learn the features about the finite one-dimensional (1D) Su-Schrieffer-Heeger (SSH) chain efficiently and classify the topological classes due to nonlinear dimensional reduction [45, 46]. Then, based on the real space descriptions, we successfully demonstrate the unsupervised clustering of several topological phononics cases: (1) disordered phononic SSH chain with random couplings; (2) Amorphous phononic systems with non-zero local Chern number; (3) Higher-order phononic models. (4) Non-Hermitian phononic chain with random dissipation terms. These phononic systems are mapped into points of the manifold space with reduced dimensions based on real space features, and are thus conveniently classified into different groups associated with different topological properties.

Let us introduce the real-space descriptors of phononic systems. The dynamic equations of phononic system can be written as $\hat{H}|\psi_l\rangle = \Omega_l|\psi_l\rangle$, where ψ_l means the l -th mode eigenstate of \hat{H} with the frequency ω_l ($\Omega_l = \omega_l^2$), $l = 1, \dots, L$ with L the system size. The time-reversal counterpart will be $\hat{H}^\dagger|\varphi_l\rangle = \Omega_l^*|\varphi_l\rangle$. Therefore, the projection operator \hat{P} of cut-off frequency ω_c is introduced, as [41–44, 47, 48]:

$$\hat{P} = \sum_{\omega_l \leq \omega_c} |\psi_l\rangle\langle\varphi_l|. \quad (1)$$

When the system is Hermitian $\hat{H} = \hat{H}^\dagger$, $\langle\varphi_l| = \langle\psi_l|$. \hat{P} describes the responses and correlations between the phononic oscillators, $P_{ij} = \langle x_j|\hat{P}|x_i\rangle$, playing the role of Green's function. When considering the infinite system with peri-

odic Bloch boundary conditions, the \hat{P} for m -th band can be represented as the sum of Bloch wave functions $\tilde{\psi}_{m\mathbf{k}}$: $\hat{P} = \frac{V}{(2\pi)^3} \int_{\text{BZ}} d\mathbf{k} |\tilde{\psi}_{m\mathbf{k}}\rangle \langle \tilde{\psi}_{m\mathbf{k}}|$, V is the volume [41]. We introduce Gaussian kernel with controlled variance ε to define the similarity between samples n and n' :

$$K_\varepsilon(n, n') = \exp\left(-\frac{\|\hat{P}_n - \hat{P}_{n'}\|^2}{2\varepsilon L^2}\right), \quad (2)$$

where \hat{P}_n is a $L \times L$ matrix ($n \in N$), denoting the \hat{P} of the n -th sample in a set of N different realizations of the Hamiltonian parameters. $\|\cdot\|$ is Taxicab \mathbb{L}^1 -norm distance, $\|A\| = \sum_i \sum_j |A_{ij}|$. We can see that Eq. (2) reflects the similarity by calculating the projection operator between two phononic samples n and n' such that $K_\varepsilon(n, n') \approx 1$ when \hat{P}_n can transform into $\hat{P}_{n'}$ with small deformation. If considering the topological invariant v that is function of \hat{P} and $v(\hat{P} + \Delta\hat{P}) \approx v(\hat{P}) + \frac{\partial v(\hat{P})}{\partial \hat{P}} \Delta\hat{P}$, the difference between different \hat{P} will be responsible for classifying the topological properties $v(\hat{P})$, namely $|v(\hat{P}_n) - v(\hat{P}_{n'})| \propto \|\hat{P}_n - \hat{P}_{n'}\|$. Different topological classes with distinct invariants will have small similarity K_ε .

We adopt the typical manifold learning algorithm: diffusion map [45, 46, 49, 50], which has been successfully applied for the phase detection and classification of quantum spin systems [37] based on probabilistic transition processes. The diffusion process is defined by the local probability transition matrix $T_{n,n'} = \frac{1}{Z_n} K_\varepsilon(n, n')$, where $Z_n = \sum_{n'=1}^N K_\varepsilon(n, n')$ is the normalization term guaranteeing the probability conservation $\sum_{n'} T_{n,n'} = 1$. The global diffusion distance between sample n and n' after t steps can be described by $d_t(n, n') \equiv \sum_{n''} \frac{1}{Z_{n''}} |T_{n,n''}^t - T_{n',n''}^t|^2 = \sum_{j=1}^{N-1} \lambda_j^{2t} |(\phi_j)_n - (\phi_j)_{n'}|^2 \geq 0$, where the ϕ_j are the j -th right eigenvectors of \hat{T} , $\hat{T}\phi_j = \lambda_j\phi_j$, with the ordered eigenvalues $\lambda_{N-1} \leq \dots \leq \lambda_2 \leq \lambda_1 \leq 1 = \lambda_0$. The $j = 0$ diffusion mode does not contribute since it is a constant vector. It is clear that after long time diffusion $t \rightarrow \infty$, the first few components ϕ_j with largest eigenvalues λ_j will dominate, which means that we only need a few components ϕ_j to represent the samples well so as to reduce the dimension. In particular, the number of the top-ranked largest eigenvalues λ_j could determine the number of topological clusters without knowing a priori knowledge [49, 50].

Topological phonics with random couplings. We use the finite 1D SSH phononic chain model [2] to demonstrate the unsupervised clustering of topological phonics in Fig. 1(a). The dynamic equation can be written as:

$$\begin{aligned} m \frac{\partial^2}{\partial t^2} a_i &= -\kappa_1(a_i - b_{i-1}) + \kappa_2(b_i - a_i), \\ m \frac{\partial^2}{\partial t^2} b_i &= -\kappa_2(b_i - a_i) + \kappa_1(a_{i+1} - b_i), \end{aligned} \quad (3)$$

where a_i and b_i are the displacements of two atoms in the i -th unit cell from their equilibrium positions, the elastic constants $\kappa_1 = \kappa_0\delta$, $\kappa_2 = \kappa_0(1 - \delta)$, the κ_0 is a constant spring

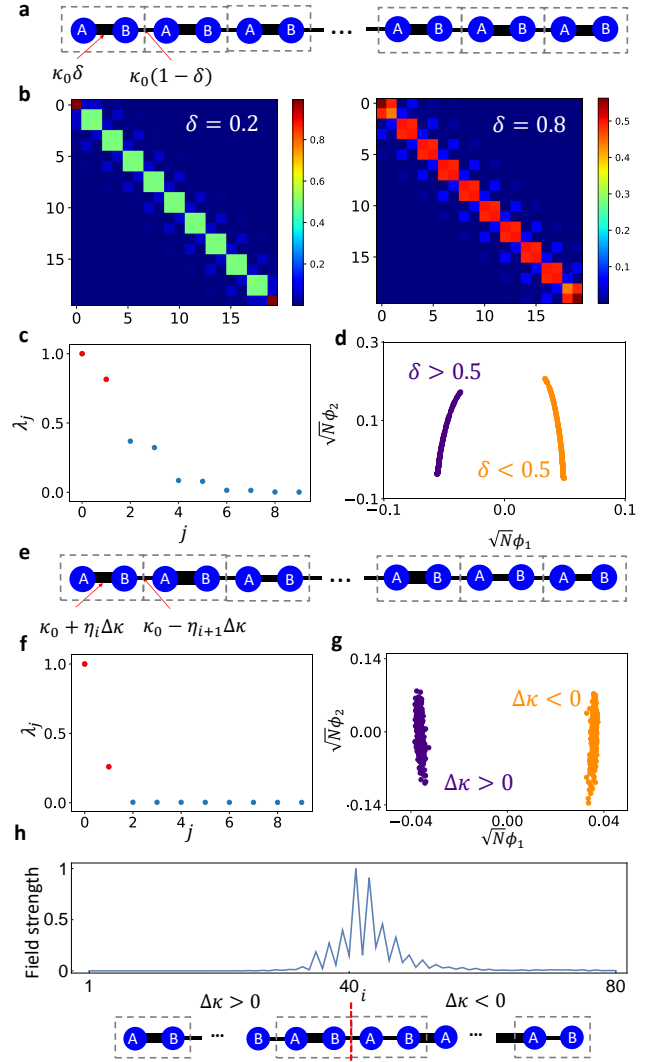


FIG. 1. The unsupervised clustering of 1D phononic SSH model with projection operator \hat{P} . **a**, the SSH chain with finite size $L = 20$, mass $m = 1.0$, spring constant $\kappa_0 = 1.0$, and $\delta \in (0, 1)$. The gray blocks indicate the unit cells. **b**, the projection operator matrix P_{ij} for the cases $\delta = 0.2$ and $\delta = 0.8$. **c**, the first 10 largest eigenvalues λ_j with $\varepsilon = 0.2$, $N = 1000$, $\omega_c = \sqrt{\kappa_0/m} = 1.0$. **d**, different topological classes are classified unsupervisedly, which coincides with the topological transition ($\delta = 0.5$) in phononic SSH model. **e**, disordered phononic SSH chain with random elastic constants, where the bias $\Delta\kappa \in (-0.75, 0.75)$ and the spatially dependent random number $\eta_i \in (0, 1)$. **f**, the first 10 largest eigenvalues λ_j with $\varepsilon = 1.0$, $N = 1000$, $\omega_c = 1.4$. **g**, different topological classes can still be well classified, even the systems are disordered by noisy couplings. **h**, the topological interface mode emerges between two random phononic chains with opposite signs of $\Delta\kappa$ ($\Delta\kappa = 0.72$ and $\Delta\kappa = -0.54$), and $L = 40$. The field strength means the absolute amplitude of displacements. (More details in Supplement.)

constant and the random number $\delta \in (0, 1)$. The calculated projection operator \hat{P} for the different δ will have some different features as shown in Fig. 1(b), which can be captured and learnt unsupervisedly by the manifold learning. Following the scheme described above on the dataset $\{\hat{P}_n\}$, we can see that

there is a second high value ($j = 1$) in Fig. 1(c), which means that the connections of samples can be reflected by the ϕ_1 . If we assign all the samples in the manifold space ϕ_1 and ϕ_2 in Fig. 1(d), we can see obviously the samples could be classified into two different groups according to the δ , with the threshold value $\delta = 0.5$, coinciding with the topological transition of SSH model. For SSH chain model, the winding number of this system can be calculated by [51]: $v = \frac{1}{2\pi i} \int_{-\pi/a}^{\pi/a} dk q^{-1} \partial_k q$, where $q = \kappa_1 + \kappa_2 e^{ika}$, which will be $v = 1$ for $\kappa_1 < \kappa_2$ ($\delta < 0.5$), $v = 0$ for $\kappa_1 > \kappa_2$ ($\delta > 0.5$).

We introduce random elastic constants in the 1D SSH-like phononic chain, as shown in Fig. 1(e). The calculated eigenvalues λ_j and the manifold space $\{\phi_j\}$ in Fig. 1(f,g) show that the samples can be also clustered well by our scheme, which resembles the topological transition in standard SSH phononic model for opposite $\Delta\kappa$. The topologically induced interface states for two disordered phononic chains with opposite signs of $\Delta\kappa$ is clearly shown in Fig. 1(h). The successful unsupervised clustering for disordered valley Hall states in 2D honeycomb phononic lattices with random mass biases can be found in Supplement.

Amorphous topological phononics insulators. Recently, the amorphous phononic lattice from random point sets has shown non-trivial topological properties and robust edge states, which demonstrates that the local interactions and local geometry arrangements are sufficient to generate chiral edge modes [47, 48], as shown in Fig. 2. The amorphous phononic topological systems are constructed by gyroscopes that are linked by springs [47], of which the topological properties can be adjusted by the geometric structures and the amorphous types. Because the sample structures are geometrically different due to the randomness, we exploit a coarse-grained mapping from the arbitrary amorphous structures into a uniform space for building uniform descriptions, as shown in Fig. 2(a): mapping the average displacement field of oscillators in the dotted block of the real space into the coarse-grained space, and then construct the \hat{P}^r based on the reduced uniform space.

Based on the dataset $\{\hat{P}_n^r\}$, we calculate eigenvalues λ_j associated with the manifold space $\{\phi_j\}$ in Fig. 2(b,c). We can see the samples can be clustered into three different groups, coinciding with the topological classes of amorphous phononics. For amorphous topological phononics insulators, the local Chern number v is responsible for describing the topological properties [44, 47]: $v = \sum_{i \in A} \sum_{j \in B} \sum_{k \in C} P_{ij} P_{jk} P_{ki} - P_{ik} P_{kj} P_{ji}$, where A, B and C is three areas around the positions (See Supplementary). As further demonstrated in Fig. 2(d), two different amorphous phononic topological insulators in samples classified by our scheme indeed show opposite chiral edge modes, with opposite local Chern numbers $v = \pm 1$. The samples in the third group do not show any chiral edge mode, corresponding to the trivial topology with $v = 0$.

Higher order topological phononics. Besides these $(d-1)$ topological properties in d dimension systems, the higher-order topological states ($d-2$ or $d-3$) are attracting much attention [6, 7, 15, 53–55]. Some higher-order topological

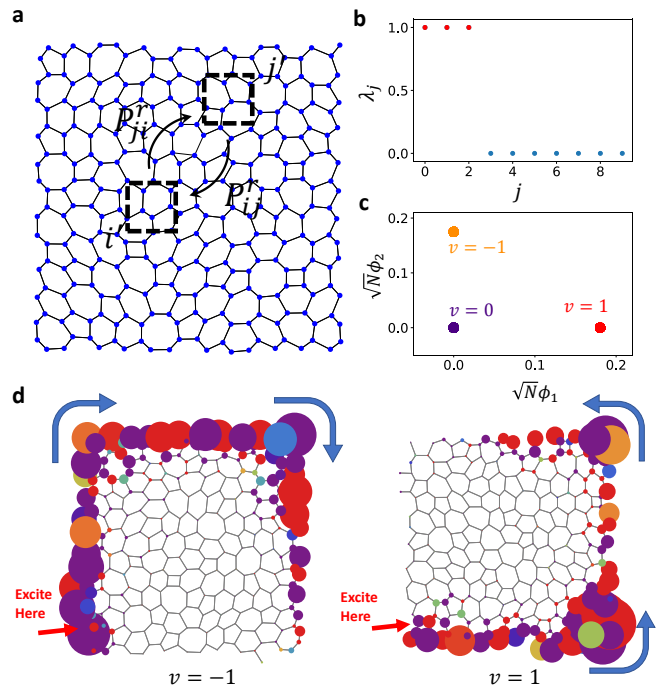


FIG. 2. The unsupervised learning of amorphous topological phononics. **a**, the demonstration of the amorphous structure, constructed by connecting adjacent centroids of Delaunay triangulation mesh [52]. The system has size $L = 130 \sim 150$. The projection operator is constructed in the coarse-grained space by averaging displacement field of oscillators in the dotted block of the original space. The reduced dimension is $L_r = 10 \times 10 = 100$. **b**, the first 10 largest eigenvalues λ_j with $\varepsilon = 0.2$, $N = 300$, $\omega_c = 1.0$. **c**, different classes that are classified unsupervisedly can coincide with different local Chern numbers v . The numbers of samples for $v = (0, -1, 1)$ are 107, 93, 100, respectively. **d**, the chiral edge modes in amorphous topological phononics with different local Chern number $v = \pm 1$. The amplitude and phase of phononic field are represented by the radius and colors (from blue to red) of the disks.

phononics can be described by the quantized shift of the Wannier center that is related to the Berry connection [6, 55]. The higher-order topological phononics can be constructed by the continuum phononic systems and the dynamic equations can be approximately written as $\ddot{x}_i = D_{ij} x_j$ around the resonant frequency ω_0 [15, 56], where D_{ij} is the effective coupling between the oscillator x_i and the oscillator x_j .

The unsupervised learning of the quadrupole higher-order topological insulator (HOTI) is demonstrated in Fig. 3(a). From the eigenvalues λ_j associated with the manifold space $\{\phi_j\}$ in Fig. 3(b,c), we can see that the N samples can be classified unsupervisedly by the threshold value $\delta = 0.67$. This value deviates from the theoretical one $\delta = 0.5$ predicted in Bloch-momentum space analysis [15, 53], due to the finite size effect. As shown in Fig. 3(d), for the finite system, the topological transition point δ , where the corner states emerge and the frequencies become degenerate at the resonant frequency (ω_0 , as the effective zero energy) will shift from theoretical value 0.5 to 0.67. This is because the ‘‘corner’’ states, although decay spatially, will interact with each other when

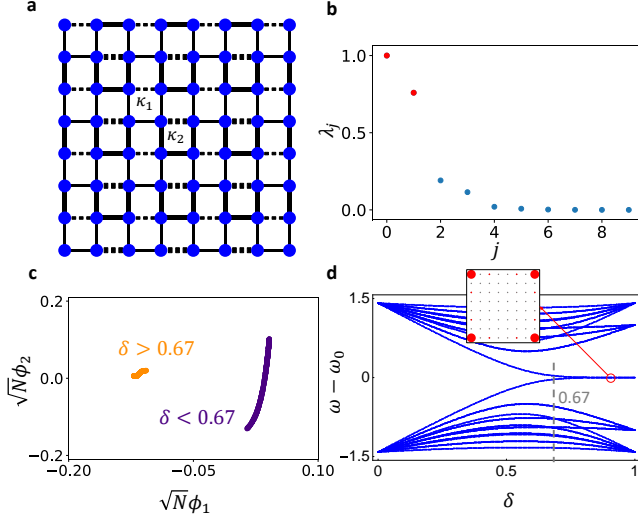


FIG. 3. The unsupervised clustering of higher-order topological phononics. **a**, the quadrupole higher-order topological models with coupling strength $\kappa_1 = \kappa_0(1 - \delta)$ and $\kappa_2 = \kappa_0\delta$, $\delta \in (0, 1)$. The dotted line means the negative counterpart. $L = 8 \times 8 = 64$. **b**, the first 10 largest eigenvalues λ_j with $\varepsilon = 1.0$, $N = 500$, $\omega_c = \omega_0$. **c**, the structures are well classified into topological classes, corresponding to different value groups of δ . **d**, the energy-levels as a function of δ shows that the unsupervised learning can predict the higher-order topological transition, even at the finite size. Inset shows the quadrupole corner states of the higher-order topological phononics.

the system size is finite. A perfect phase transition requires a clear separation of those corner states, which will be achieved when further increase δ to 0.67. This finite size effect of HOTI classification can not be found before in the Bloch picture for periodic infinite systems. The unsupervised learning for HOTI in phononic Kagome lattices can be found in Supplement.

Non-Hermitian topological phononics. The topological properties in non-Hermitian systems without time-reversal symmetry are very important [57–65]. The non-Hermitian feature can be originated from many aspects [66], such as the non-reciprocal coupling between the nearest oscillators [67], the non-zero dissipation bias, or the complex on-site potentials [60, 68]. Mathematically, the non-Hermitian system will have complex eigenfrequencies and non-orthogonal eigenvectors [69]. Some Bloch analysis have been applied for non-Hermitian systems and found that the exception points play important roles for the topological origin [60, 65]. However, the non-Bloch analysis also states the non-Hermitian skin (surface) effect and describes the edge modes as well [62, 63]. Thus, the non-Hermitian topological invariants are not clear in general and still being under explorations [62–65, 70].

Here, we consider the 1D phononic lattice with different and random dissipation terms due to the non-zero viscosity $\tau_{A/B} \neq 0$, shown in Fig. 4(a). The dynamic equation can be

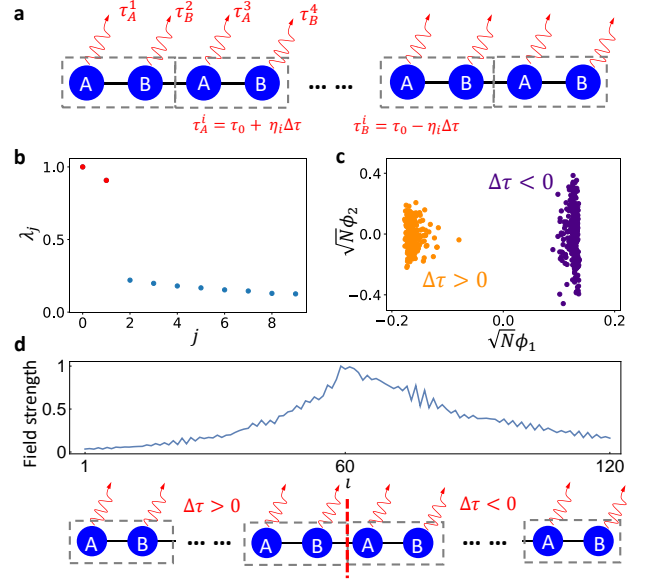


FIG. 4. The unsupervised clustering of 1D non-Hermitian phononic chain. **a**, the A/B oscillators have random dissipation losses, with alternatively large and small dissipation values $\tau_{A/B}^i = \tau_0 \pm \eta_i \Delta\tau$, respectively. The length size $L = 20$, the mass $m = 1.0$, the viscosity $\tau_0 = 1.0$, the viscosity bias $\Delta\tau \in (-0.5, 0.5)$ and the random number $\eta_i \in (0, 1)$. **b**, the first 10 largest eigenvalues λ_j with $\varepsilon = 1.0$, $N = 500$, $\omega_c = 1.35$. **c**, different classes are classified unsupervisedly, which coincides with the fact that the cases of $\tau_A > \tau_B$ ($\Delta\tau > 0$) and $\tau_A < \tau_B$ ($\Delta\tau < 0$) are topologically distinct. **d**, the topological interface mode emerges between two non-Hermitian random phononic chains with opposite signs of $\Delta\tau$ ($\Delta\tau = 0.4$ and $\Delta\tau = -0.24$), and $L = 60$.

written as:

$$\begin{aligned} m \frac{\partial^2}{\partial t^2} a_i + \tau_A^i \frac{\partial}{\partial t} a_i &= -\kappa(a_i - b_{i-1}) + \kappa(b_i - a_i), \\ m \frac{\partial^2}{\partial t^2} b_i + \tau_B^{i+1} \frac{\partial}{\partial t} b_i &= -\kappa(b_i - a_i) + \kappa(a_{i+1} - b_i), \end{aligned} \quad (4)$$

where $\tau_{A/B}^i$ is the different and random dissipation viscosity terms of A/B oscillators for the different i -th oscillator. From the eigenvalues λ_j associated with the manifold space $\{\phi_j\}$ in Fig. 4(b,c), we can see the N samples are clustered into two different groups: $\Delta\tau > 0$ or $\Delta\tau < 0$ corresponding to the case $\tau_A > \tau_B$ or $\tau_A < \tau_B$, which coincides with the fact that the cases of $\tau_A > \tau_B$ and $\tau_A < \tau_B$ are topologically distinct. As a result, the topological interface state emerges at the interface between two topologically different random non-Hermitian chains with opposite signs of $\Delta\tau$, as shown in Fig. 4(d).

To summarize, we have exemplified the function of unsupervised manifold clustering of topological phononics. Several main difficulties of topological phononics including the spatial randomness, the amorphous non-periodic structures and the non-Hermitian dissipations have been discussed. The unsupervised manifold learning have achieved the efficient non-linear dimension reductions, which would map the phononic systems into the manifold space based on their

features in the real space and then cluster them into different groups associated with different topological properties. Our work would be used to explore diverse topological phononics before defining or introducing topological invariants, which is meaningful for not only theoretical understandings but also experimental detections, especially for the random, non-Hermitian and out-of-equilibrium open phononic systems [62–65].

We acknowledge the support from the National Key Research Program of China (No. 2016YFA0301101), National Natural Science Foundation of China (No. 11935010, No. 11775159 and No. 61621001), the Shanghai Science and Technology Committee (Nos. 18ZR1442800 and 18JC1410900), the Opening Project of Shanghai Key Laboratory of Special Artificial Microstructure Materials and Technology.

* Corresponding Email: Xonics@tongji.edu.cn

- [1] Yizhou Liu, Yong Xu, and Wenhui Duan, “Berry phase and topological effects of phonons,” *Natl. Sci. Rev.* **5**, 314–316 (2017).
- [2] Sebastian D Huber, “Topological mechanics,” *Nat. Phys.* **12**, 621 (2016).
- [3] Lifa Zhang, Jie Ren, Jian-Sheng Wang, and Baowen Li, “Topological nature of the phonon hall effect,” *Phys. Rev. Lett.* **105**, 225901 (2010).
- [4] Guancong Ma and Ping Sheng, “Acoustic metamaterials: From local resonances to broad horizons,” *Sci. Adv.* **2**, e1501595 (2016).
- [5] Hao Ge, Min Yang, Chu Ma, Ming-Hui Lu, Yan-Feng Chen, Nicholas Fang, and Ping Sheng, “Breaking the barriers: advances in acoustic functional materials,” *Natl. Sci. Rev.* **5**, 159–182 (2017).
- [6] Haoran Xue, Yahui Yang, Fei Gao, Yidong Chong, and Baile Zhang, “Acoustic higher-order topological insulator on a kagome lattice,” *Nat. Mater.* **18**, 108 (2019).
- [7] Xiujuan Zhang, Hai-Xiao Wang, Zhi-Kang Lin, Yuan Tian, Biye Xie, Ming-Hui Lu, Yan-Feng Chen, and Jian-Hua Jiang, “Second-order topology and multidimensional topological transitions in sonic crystals,” *Nat. Phys.* **15**, 582 (2019).
- [8] M Zahid Hasan and Charles L Kane, “Colloquium: topological insulators,” *Rev. Mod. Phys.* **82**, 3045 (2010).
- [9] Di Xiao, Ming-Che Chang, and Qian Niu, “Berry phase effects on electronic properties,” *Rev. Mod. Phys.* **82**, 1959 (2010).
- [10] Arun Bansil, Hsin Lin, and Tanmoy Das, “Colloquium: Topological band theory,” *Rev. Mod. Phys.* **88**, 021004 (2016).
- [11] Roman Süssstrunk and Sebastian D Huber, “Observation of phononic helical edge states in a mechanical topological insulator,” *Science* **349**, 47–50 (2015).
- [12] Pai Wang, Ling Lu, and Katia Bertoldi, “Topological phononic crystals with one-way elastic edge waves,” *Phys. Rev. Lett.* **115**, 104302 (2015).
- [13] Mou Yan, Jiuyang Lu, Feng Li, Weiyin Deng, Xueqin Huang, Jiahong Ma, and Zhengyou Liu, “On-chip valley topological materials for elastic wave manipulation,” *Nat. Mater.* **17**, 993 (2018).
- [14] Meng Xiao, Wen-Jie Chen, Wen-Yu He, and Che Ting Chan, “Synthetic gauge flux and weyl points in acoustic systems,” *Nat. Phys.* **11**, 920 (2015).
- [15] Marc Serra-Garcia, Valerio Peri, Roman Süssstrunk, Osama R Bilal, Tom Larsen, Luis Guillermo Villanueva, and Sebastian D Huber, “Observation of a phononic quadrupole topological insulator,” *Nature* **555**, 342 (2018).
- [16] Yizhou Liu, Chao-Sheng Lian, Yang Li, Yong Xu, and Wenhui Duan, “Pseudospins and topological effects of phonons in a kekulé lattice,” *Phys. Rev. Lett.* **119**, 255901 (2017).
- [17] S Hossein Mousavi, Alexander B Khanikaev, and Zheng Wang, “Topologically protected elastic waves in phononic metamaterials,” *Nat. Commun.* **6**, 8682 (2015).
- [18] Cheng He, Xu Ni, Hao Ge, Xiao-Chen Sun, Yan-Bin Chen, Ming-Hui Lu, Xiao-Ping Liu, and Yan-Feng Chen, “Acoustic topological insulator and robust one-way sound transport,” *Nat. Phys.* **12**, 1124 (2016).
- [19] Hailong He, Chunyin Qiu, Liping Ye, Xiangxi Cai, Xiyang Fan, Manzhou Ke, Fan Zhang, and Zhengyou Liu, “Topological negative refraction of surface acoustic waves in a weyl phononic crystal,” *Nature* **560**, 61 (2018).
- [20] Pengfei Zhang, Huitao Shen, and Hui Zhai, “Machine learning topological invariants with neural networks,” *Phys. Rev. Lett.* **120**, 066401 (2018).
- [21] Jordan Venderley, Vedika Khemani, and Eun-Ah Kim, “Machine learning out-of-equilibrium phases of matter,” *Phys. Rev. Lett.* **120**, 257204 (2018).
- [22] John Peurifoy, Yichen Shen, Li Jing, Yi Yang, Fidel Cano-Renteria, Brendan G DeLacy, John D Joannopoulos, Max Tegmark, and Marin Soljačić, “Nanophotonic particle simulation and inverse design using artificial neural networks,” *Sci. Adv.* **4**, eaar4206 (2018).
- [23] Pankaj Mehta, Marin Bukov, Ching-Hao Wang, Alexandre GR Day, Clint Richardson, Charles K Fisher, and David J Schwab, “A high-bias, low-variance introduction to machine learning for physicists,” *Physics Reports* **810**, 1 – 124 (2019).
- [24] Vedran Dunjko and Hans J Briegel, “Machine learning & artificial intelligence in the quantum domain: a review of recent progress,” *Reports on Progress in Physics* **81**, 074001 (2018).
- [25] Giuseppe Carleo, Ignacio Cirac, Kyle Cranmer, Laurent Daudet, Maria Schuld, Naftali Tishby, Leslie Vogt-Maranto, and Lenka Zdeborová, “Machine learning and the physical sciences,” *Rev. Mod. Phys.* **91**, 045002 (2019).
- [26] Juan Carrasquilla and Roger G Melko, “Machine learning phases of matter,” *Nat. Phys.* **13**, 431 (2017).
- [27] Yi Zhang and Eun-Ah Kim, “Quantum loop topography for machine learning,” *Phys. Rev. Lett.* **118**, 216401 (2017).
- [28] Evert PL Van Nieuwenburg, Ye-Hua Liu, and Sebastian D Huber, “Learning phase transitions by confusion,” *Nat. Phys.* **13**, 435 (2017).
- [29] Giuseppe Carleo and Matthias Troyer, “Solving the quantum many-body problem with artificial neural networks,” *Science* **355**, 602–606 (2017).
- [30] Laura Piloizzi, Francis A Farrelly, Giulia Marcucci, and Claudio Conti, “Machine learning inverse problem for topological photonics,” *Commun. Phys.* **1**, 57 (2018).
- [31] Yang Long, Jie Ren, Yunhui Li, and Hong Chen, “Inverse design of photonic topological state via machine learning,” *Appl. Phys. Lett.* **114**, 181105 (2019).
- [32] Dianjing Liu, Yixuan Tan, Erfan Khoram, and Zongfu Yu, “Training deep neural networks for the inverse design of nanophotonic structures,” *ACS Photonics* **5**, 1365–1369 (2018).
- [33] Wei Ma, Feng Cheng, and Yongmin Liu, “Deep-learning-enabled on-demand design of chiral metamaterials,” *ACS Nano* **12**, 6326–6334 (2018).
- [34] Zhaocheng Liu, Dayu Zhu, Sean P Rodrigues, Kyu-Tae Lee,

- and Wenshan Cai, “Generative model for the inverse design of metasurfaces,” *Nano Lett.* **18**, 6570–6576 (2018).
- [35] Lei Wang, “Discovering phase transitions with unsupervised learning,” *Phys. Rev. B* **94**, 195105 (2016).
- [36] Sebastian J. Wetzel, “Unsupervised learning of phase transitions: From principal component analysis to variational autoencoders,” *Phys. Rev. E* **96**, 022140 (2017).
- [37] Joaquin F Rodriguez-Nieva and Mathias S Scheurer, “Identifying topological order through unsupervised machine learning,” *Nat. Phys.* **15**, 790–795 (2019).
- [38] Anders Andreassen, Ilya Feige, Christopher Frye, and Matthew D Schwartz, “Junipr: a framework for unsupervised machine learning in particle physics,” *Eur. Phys. J. C* **79**, 102 (2019).
- [39] Pierre Baldi, Peter Sadowski, and Daniel Whiteson, “Searching for exotic particles in high-energy physics with deep learning,” *Nat. Commun.* **5**, 4308 (2014).
- [40] Vahe Tshitoyan, John Dagdelen, Leigh Weston, Alexander Dunn, Ziqin Rong, Olga Kononova, Kristin A Persson, Gerbrand Ceder, and Anubhav Jain, “Unsupervised word embeddings capture latent knowledge from materials science literature,” *Nature* **571**, 95 (2019).
- [41] Nicola Marzari, Arash A Mostofi, Jonathan R Yates, Ivo Souza, and David Vanderbilt, “Maximally localized wannier functions: Theory and applications,” *Rev. Mod. Phys.* **84**, 1419 (2012).
- [42] Alexey A Soluyanov and David Vanderbilt, “Wannier representation of z_2 topological insulators,” *Phys. Rev. B* **83**, 035108 (2011).
- [43] Raffaello Bianco and Raffaele Resta, “Mapping topological order in coordinate space,” *Phys. Rev. B* **84**, 241106 (2011).
- [44] Alexei Kitaev, “Anyons in an exactly solved model and beyond,” *Annals of Physics* **321**, 2–111 (2006).
- [45] Joshua B Tenenbaum, Vin De Silva, and John C Langford, “A global geometric framework for nonlinear dimensionality reduction,” *Science* **290**, 2319–2323 (2000).
- [46] Sam T Roweis and Lawrence K Saul, “Nonlinear dimensionality reduction by locally linear embedding,” *Science* **290**, 2323–2326 (2000).
- [47] Noah P Mitchell, Lisa M Nash, Daniel Hexner, Ari M Turner, and William TM Irvine, “Amorphous topological insulators constructed from random point sets,” *Nat. Phys.* **14**, 380 (2018).
- [48] Adhip Agarwala and Vijay B Shenoy, “Topological insulators in amorphous systems,” *Phys. Rev. Lett.* **118**, 236402 (2017).
- [49] Ronald R Coifman and Stéphane Lafon, “Diffusion maps,” *Appl. Comput. Harmon. Anal.* **21**, 5–30 (2006).
- [50] Ronald R Coifman, Stéphane Lafon, Ann B Lee, Mauro Maggioni, Boaz Nadler, Frederick Warner, and Steven W Zucker, “Geometric diffusions as a tool for harmonic analysis and structure definition of data: Diffusion maps,” *Proc. Natl. Acad. Sci. U. S. A.* **102**, 7426–7431 (2005).
- [51] Roman Süssstrunk and Sebastian D Huber, “Classification of topological phonons in linear mechanical metamaterials,” *Proc. Natl. Acad. Sci. U. S. A.* **113**, E4767–E4775 (2016).
- [52] Marian Florescu, Salvatore Torquato, and Paul J Steinhardt, “Designer disordered materials with large, complete photonic band gaps,” *Proc. Natl. Acad. Sci. U. S. A.* **106**, 20658–20663 (2009).
- [53] Wladimir A Benalcazar, B Andrei Bernevig, and Taylor L Hughes, “Quantized electric multipole insulators,” *Science* **357**, 61–66 (2017).
- [54] Xiujuan Zhang, Bi-Ye Xie, Hong-Fei Wang, Xiangyuan Xu, Yuan Tian, Jian-Hua Jiang, Ming-Hui Lu, and Yan-Feng Chen, “Dimensional hierarchy of higher-order topology in three-dimensional sonic crystals,” *Nat. Commun.* **10**, 1–10 (2019).
- [55] Xiang Ni, Matthew Weiner, Andrea Alù, and Alexander B Khanikaev, “Observation of higher-order topological acoustic states protected by generalized chiral symmetry,” *Nat. Mater.* **18**, 113 (2019).
- [56] Kathryn H Matlack, Marc Serra-Garcia, Antonio Palermo, Sebastian D Huber, and Chiara Daraio, “Designing perturbative metamaterials from discrete models,” *Nat. Mater.* **17**, 323 (2018).
- [57] Sebastian Diehl, Enrique Rico, Mikhail A Baranov, and Peter Zoller, “Topology by dissipation in atomic quantum wires,” *Nat. Phys.* **7**, 971 (2011).
- [58] Kun Ding, Guancong Ma, Meng Xiao, Z. Q. Zhang, and C. T. Chan, “Emergence, coalescence, and topological properties of multiple exceptional points and their experimental realization,” *Phys. Rev. X* **6**, 021007 (2016).
- [59] Julia M Zeuner, Mikael C Rechtsman, Yonatan Plotnik, Yaakov Lumer, Stefan Nolte, Mark S Rudner, Mordechai Segev, and Alexander Szameit, “Observation of a topological transition in the bulk of a non-hermitian system,” *Phys. Rev. Lett.* **115**, 040402 (2015).
- [60] Daniel Leykam, Konstantin Y Bliokh, Chunli Huang, Yi Dong Chong, and Franco Nori, “Edge modes, degeneracies, and topological numbers in non-hermitian systems,” *Phys. Rev. Lett.* **118**, 040401 (2017).
- [61] Kun Ding, Guancong Ma, Z. Q. Zhang, and C. T. Chan, “Experimental demonstration of an anisotropic exceptional point,” *Phys. Rev. Lett.* **121**, 085702 (2018).
- [62] Huitao Shen, Bo Zhen, and Liang Fu, “Topological band theory for non-hermitian hamiltonians,” *Phys. Rev. Lett.* **120**, 146402 (2018).
- [63] Shunyu Yao and Zhong Wang, “Edge states and topological invariants of non-hermitian systems,” *Phys. Rev. Lett.* **121**, 086803 (2018).
- [64] Kinjal Dasbiswas, Kranthi K Mandadapu, and Suriyanarayanan Vaikuntanathan, “Topological localization in out-of-equilibrium dissipative systems,” *Proc. Natl. Acad. Sci. U. S. A.* **115**, E9031–E9040 (2018).
- [65] Zongping Gong, Yuto Ashida, Kohei Kawabata, Kazuaki Takasan, Sho Higashikawa, and Masahito Ueda, “Topological phases of non-hermitian systems,” *Phys. Rev. X* **8**, 031079 (2018).
- [66] Ananya Ghatak and Tanmoy Das, “New topological invariants in non-hermitian systems,” *Journal of Physics: Condensed Matter* **31**, 263001 (2019).
- [67] Tony E Lee, “Anomalous edge state in a non-hermitian lattice,” *Phys. Rev. Lett.* **116**, 133903 (2016).
- [68] Mudi Wang, Liping Ye, Johan Christensen, and Zhengyou Liu, “Valley physics in non-hermitian artificial acoustic boron nitride,” *Phys. Rev. Lett.* **120**, 246601 (2018).
- [69] Carl M Bender, “Making sense of non-hermitian hamiltonians,” *Reports on Progress in Physics* **70**, 947 (2007).
- [70] Tao Liu, Yu-Ran Zhang, Qing Ai, Zongping Gong, Kohei Kawabata, Masahito Ueda, and Franco Nori, “Second-order topological phases in non-hermitian systems,” *Phys. Rev. Lett.* **122**, 076801 (2019).